EXPERIMENTS ON STRONG ELECTROMAGNETIC INTERACTIONS WITH PLASMAS – INVESTIGATION OF NON-LINEAR PROCESSES IN LASER FUSION

A.Y. WONG, R.L. STENZEL, H.C. KIM
TRW Systems and University of California,
Los Angeles, Calif.

F.F. CHEN
University of California,
Los Angeles, Calif.
United States of America

Abstract

EXPERIMENTS ON STRONG ELECTROMAGNETIC INTERACTIONS WITH PLASMAS – INVESTIGATION OF NON-LINEAR PROCESSES IN LASER FUSION.

The large resonant response of a non-uniform plasma to an incident electromagnetic wave in the critical region $\omega_p(z_c) \approx \omega_0$ has resulted in strong non-linearities. Ponderomotive forces drive electrons and ions out from the resonant region, creating density perturbations as large as 60%. Accelerated ions gain energy by as much as $7kT_e$; while fast electrons gain energy by as much as 25 kT_e through transit-time damping. Parametric backscattering has also been observed with CO_2 radiation in a plasma well below the critical density. The threshold agrees in order of magnitude with the theory of stimulated Brillouin scattering in a finite region.

The difficulty in diagnosing the linear and non-linear processes in the small critical region $\omega_p(z_0) \approx \omega_0$ where the laser interacts strongly with plasmas has motivated our simulation experiments in the microwave and RF regimes. We have designed a large-scale plasma [1] (2 m diameter and 4 m long) in which the density gradient scale-length L (0.5-10 m) $\gg \lambda_0$ (15 cm), where λ_0 is the free-space wavelength. The following are the new important results of our experiments.

1. BEAM FOCUSING BY PLASMA REFRACTIVE EFFECTS

By mapping the spatial propagation of the EM wave along the density gradient (Fig.1) we found that the spatially decreasing plasma refractive index causes an EM beam to diverge [2] or converge by a factor of 20 db, depending on the initial beam divergence. The one-dimensional prediction of amplitude swelling based on the reduction in group velocity does not occur.

2. LARGE PLASMA ENHANCEMENTS (60 db) OF INCIDENT E FIELD

For oblique incidence of EM waves with respect to the density gradient, the component of E parallel to the density gradient can be resonantly

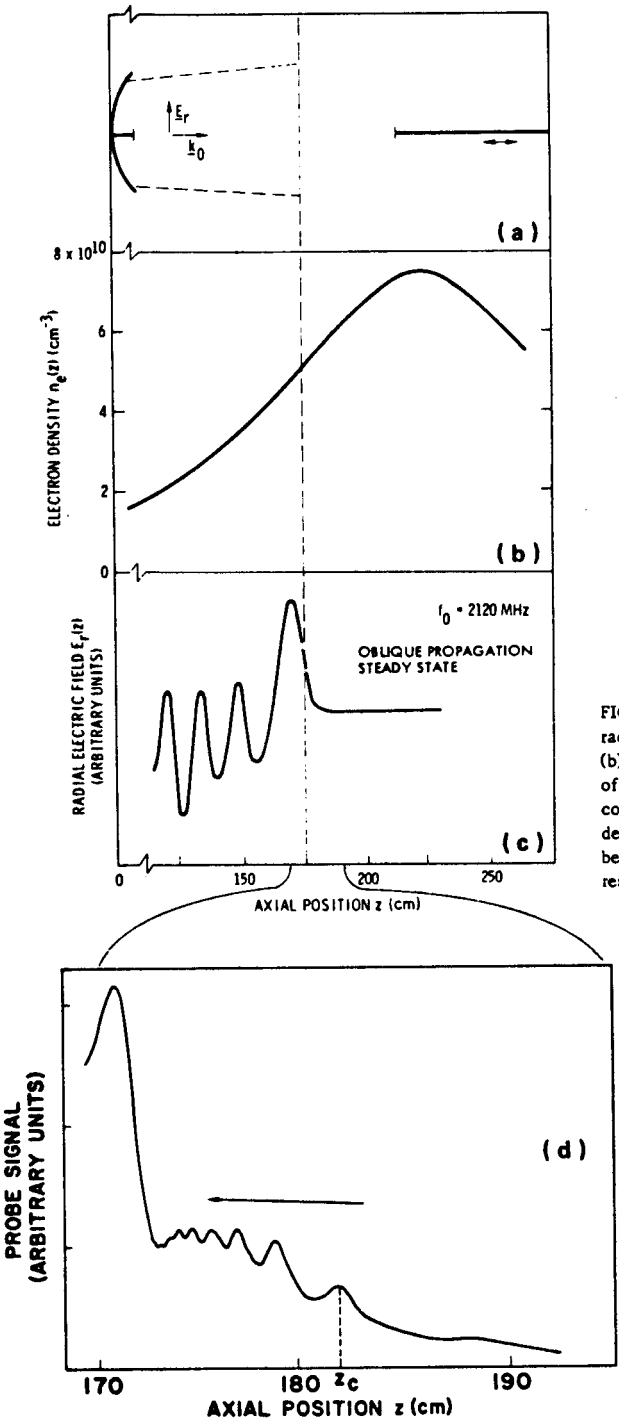

FIG.1. (a) Experimental arrangement of the radiating antenna and the detection probe; (b) axial density profile; (c) spatial dependence of the radial electric field $E_r(z)$; (d) linear converted plasma waves propagating down the density gradient towards the EM cut-off after being excited at resonant location z_c by the resonantly enhanced field E_z.

enhanced by 60 db in the critical region $\omega_p(z_c) = \omega_0$. The density gradient allows charge accumulations to occur under this enhanced driving field E_z, and electron plasma oscillations are excited, which then propagate down the density profile. Even for rather modest incident EM fields, $E^2/4\pi n_0 kT_e \gtrsim 10^{-5}$, such large resonant enhancements inside the plasma can bring about strong interactions. Two distinct types of instabilities are observed at separate locations in this non-uniform plasma, as indicated below.

3. DEVELOPMENT OF CAVITONS (DENSITY CAVITIES) [3]

This is a new kind of parametric instability in which the ponderomotive force of the localized enhanced E_z field at the resonant location $\omega_0 = \omega_p(z_c)$ generates a density cavity by first expelling the electrons and then the ions. The cavity in turn traps the RF field and causes mutual enhancement between the RF field and the density perturbation.

The experimental arrangement and the main observations [4] can be best described by the simultaneous spatial and temporal descriptions of the process in Fig.2. The short (0.4 μs) electromagnetic pulse is converted to an electrostatic pulse of high field intensity near the resonant layer $\omega_0 = \omega_p(z_0)$ as a result of the much smaller group velocity and the resonant enhancement at that layer. Observations with the aid of an ion energy analyser at several microseconds after the EM pulse show the presence of a large ion current (twice the normal saturation value) just outside the resonant region. This enhanced current is found to consist of ions of much higher energy than the ambient. This current peak is followed by a density depression ($\delta n/n = 30\%$) which is a result of the expulsion of ions from the resonant region. As this ion structure travels down the density profile, the peak consisting of a wide range of ion velocities quickly disperses, while the density cavity ("caviton") composed of background ions maintains its shape as a non-linear ion perturbation for a much longer time.

The development of this caviton is studied by a probing electron beam in a direction transverse to the axis. For a modest pump power ($E_0^2/4\pi nT_e \approx 10^{-6}$) the time- and space-resolved measurements show a simultaneous exponential growth of the internal field $\langle E_T \rangle$ and δn at the resonant location with the growth rate γ depending linearly on the pump power E_0^2. Measurements of the absolute RF field strength and density perturbation establish $\delta n \propto \langle E_T^2 \rangle$ qualitatively and $\langle E_T^2 \rangle / 8\pi n_0 kT_e \approx \delta n/n_0$ quantitatively within 30% error. $\langle E_T^2 \rangle / 8\pi n_0 kT_e$ grows to a saturated value of 25% in about 10 μs which is the typical time scale for the development of the ion density perturbation. The resonant width at this time is typically 20 Debye lengths. The behaviour of $\langle E_T^2 \rangle$ and δn after the saturation depends on the density gradient scale-length: for gentle density gradient ($k_D L > 500$), $\langle E_T \rangle$ and δn break down into several peaks and propagate out from the resonant region towards regions of higher and lower densities [5]; for a steeper density gradient ($k_D L < 500$), a short-wavelength ($k\lambda_D = 0.3$) ion acoustic wave is generated inside the density cavity and propagates down the density gradient. When the ion acoustic wave is generated, $\langle E_T^2 \rangle$ in the density cavity oscillates at the ion acoustic frequency and starts to decay to the final steady state value, approximately 1/10 of the peak value.

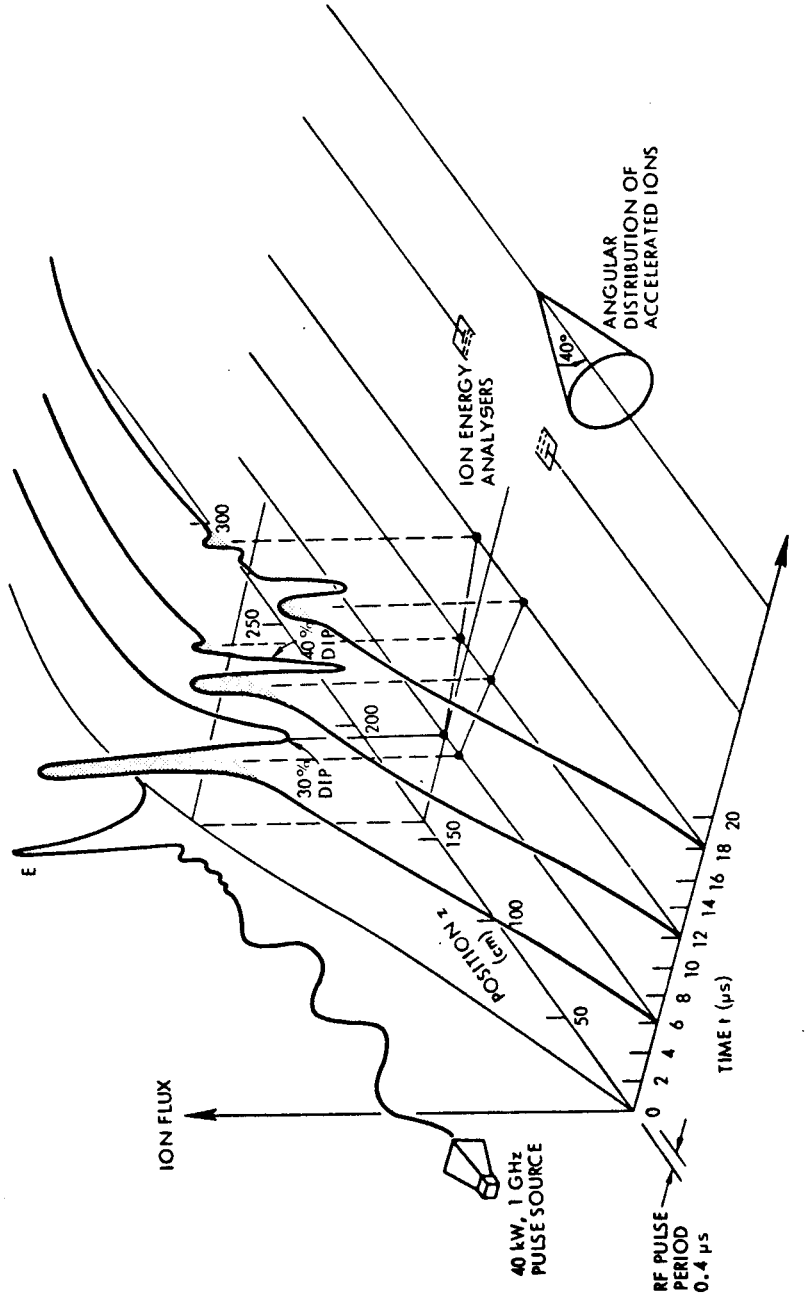

FIG. 2. Space-time representation of ion bursts (shaded) driven by the ponderomotive force. Density cavities are created as a result of ion expulsion. The polarization of ion trajectories is represented by the cone with a half-width of 40° with respect to the z-axis.

In spite of the large density perturbations, the resonant RF field keeps on growing in the vicinity (within 2 cm) of the initial resonant location, indicating that the RF field is trapped inside the density cavity. To verify this hypothesis, we turned off the RF pump abruptly and confirmed that the field inside the density cavity lasts 100 periods and is determined by the electron neutral collision rate and not by wave convection.

For a strong incident power $E_0^2/4\pi nkT_e \lesssim 10^{-2}$ the internal field $\langle E_T^2 \rangle/4\pi nkT_e$ can rise to a transient value of 10, even before the ions have sufficient time to move, and a density perturbation of 40-60% could be subsequently created. As shown in Fig.2, such a large-amplitude caviton steepens as it propagates down the density gradient.

4. PARAMETRIC DECAY INSTABILITY IN AN INHOMOGENEOUS MEDIUM

While the linear conversion and the development of cavitons originate at the resonant location, the parametric decay instability is observed to grow temporally within a limited region (0.5 cm) bounded by the electromagnetic field decay on the one side and the rise of the electrostatic field on the other, as shown in Fig.3. The frequency spectra exhibit the classical parametric form, namely a lower-frequency electronic sideband $E(\omega_0-\omega_i)$ and a low-frequency ion wave signal $n_i(\omega_i)$. Both sideband components show a stationary pattern inside the "well" and a propagating pattern outside. The inhomogeneous pump field $|E_{0z}|$ gives rise to an absolute instability situated near its minimum field strength. The group velocity of the electron sideband in both directions up and down the density gradient has been measured as 5×10^4 cm/s, which is much less than the electron thermal velocity, 6×10^7 cm/s. The slow group velocity out of the source region is a necessary condition of the absolute instability.

The instability starts with a coherent spectrum until saturation, where the waves become much less coherent and have a steady-state bandwidth of $\Delta\omega/\omega \approx 1/3$ in the ion wave spectrum. The ion wave amplitude is about 1-2%, while the electron wave amplitude is at least an order of magnitude below the resonant peak value since no significant density perturbation due to ponderomotive force is observed at the start of the parametric instabilities. We can conclude by saying that this decay instability is a much weaker non-linear phenomenon than the one in the resonant region.

5. PARTICLE ACCELERATION BY SPATIALLY LOCALIZED FIELDS

5.1. Electron acceleration

Electrons which can traverse the localized region ($20\,\lambda_D$) in about half the plasma period could gain maximum energy from the localized region. This has indeed been confirmed by our electron beam diagnostic which shows that the energy gained by a test electron is up to 50V. Only the fast electrons $(6(kT/m)^{\frac{1}{2}})$ could be accelerated significantly [6]. Our experiments show no significant increase in the bulk distribution of electrons.

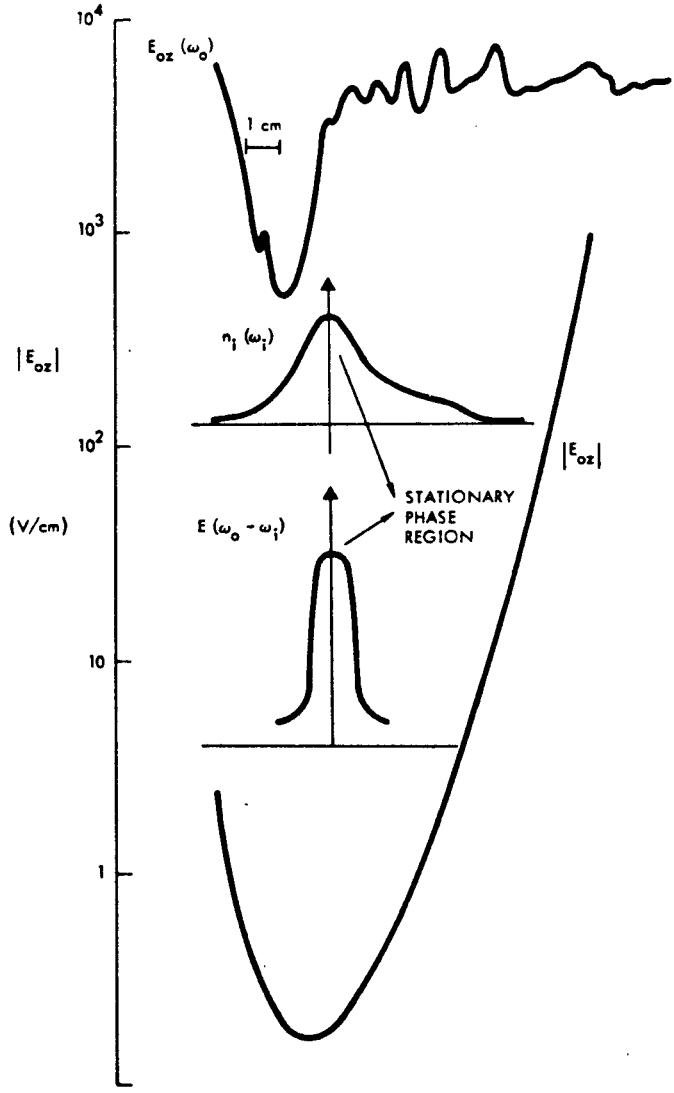

FIG.3. Locations of ion and electron sidebands $n_i(\omega_i)$ and $E(\omega_0-\omega_i)$ with respect to the linear converted waves. The plot of the absolute amplitude of the axial field $|E_z|$ shows the existence of a "well" in the pump profile.

5.2. Ion acceleration [4]

Under the highly localized electric field in Fig.2 the anharmonic motion of electrons gives rise to a time-averaged force field $-\nabla \langle E^2 \rangle / 8\pi$ (derived from the $v \cdot \nabla v$ term in the electron equation of motion) which pushes electrons down the field gradient. As the electrons are accelerated, they pull the ions with them by means of ambipolar fields.

This process is indeed confirmed by our experimental observations that the electron response comes out first from the resonant region followed by the ionic response, as monitored by a Langmuir probe and an ion energy analyser all mounted on the same movable shaft located at a distance of 2 cm. The ions eventually catch up with the electrons and travel together. Ions with energy up to 7 kT_e are detected by an ion energy analyser.

The above process requires an RF pulse of sufficient duration ($\tau > \Delta z / v_e \approx 0.1\ \mu s$) to set up the initial electron drift and displacement away from the resonant layer ($\Delta z \lesssim 2$ cm). Once such a duration is exceeded, the net electron drift and the accelerating field to pull the ions depend more on the peak RF power. We have found that the energetic ion flux bears approximately the same linear relation to the peak power, even though the pulse duration changes by a factor of 5. The insensitivity to the total energy content of the applied pulse distinguishes this process from that of turbulent wave-particle interactions; the turbulent ion-wave spectrum must depend on the energy input into the system and the pulse duration should be many times the plasma ion-wave period in order that a turbulent wave spectrum develops.

6. PARAMETRIC BACKSCATTERING OF LASER RADIATION

Stimulated Brillouin scattering (SBS) has been shown theoretically [7] and computationally [8] to be a possible source of difficulty in laser fusion, since the laser light can be reflected in the underdense region before it can be absorbed in the critical density region by parametric decay. In solid-target experiments, phenomena at $\omega = \omega_p$ and $\omega = 2\omega_p$ mask the pure SBS effect. To avoid this, our experiment is designed to have $\omega_p < \omega/2$ everywhere. The plasma is produced by a 50-μs axial discharge in a 4-kG magnetic field (Fig.4). A double-discharge CO_2 laser produces at 45-J, 100-ns FWHM pulse (Fig.5a), which is focused by a 75-cm-focal-length lens and passes through the plasma axially via hollow electrodes. Illumination and plasma parameters are fairly uniform over a focal region $0.1 \times 0.2 \times 3$ cm long. Backscattered radiation is collected from a NaCl beam-splitter, frequency-analysed by a Fabry-Perot interferometer, and focused onto a Hg:Ge detector at 4 K. The threshold of detectability is determined by diffraction at the 5-cm-diameter laser aperture and by scattering on optical surfaces.

Figure 5a shows the stray light signal in the absence of plasma. The peak power is about 50 W; the incident power is 4×10^8 W. Figure 5b shows the backscatter signal with a 30-kA discharge at 10 torr of argon; it appears as a sharp spike delayed 10-50 ns from the peak of the incident pulse. Figure 5c shows the signal at 20 torr of argon. The initial peak is shortened, and a large, unexplained reflection is observed 200-500 ns afterwards. At 20 torr it is possible that multiple ionization of argon raises ω_p above $\omega/2$. The threshold of detectability occurs at $n_0 \simeq 2 \times 10^{17}$ cm^{-3} (measured by He-Ne laser interferometry) and incident intensity $I \simeq 1.5 \times 10^{10}$ W/cm^2.

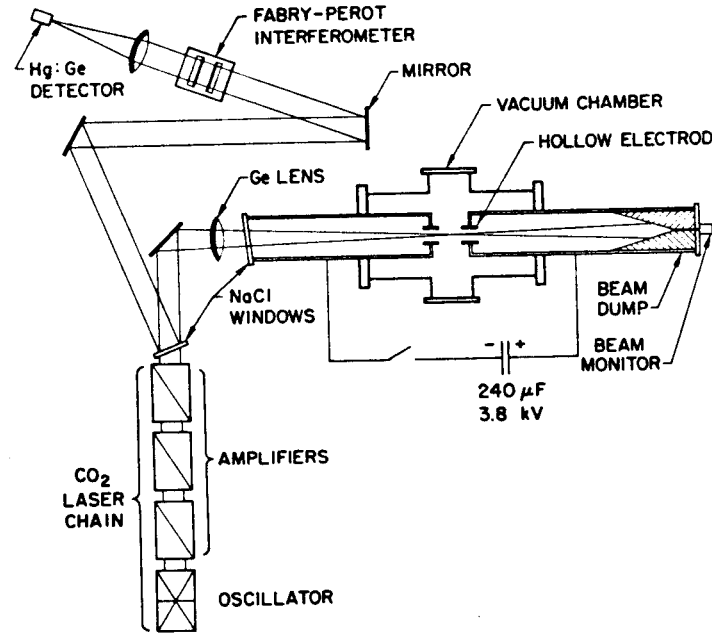

FIG.4. Schematic diagram of CO_2 backscattering experiment.

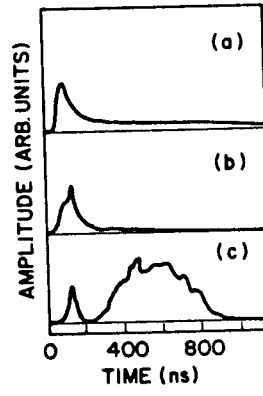

FIG.5. Typical backscattered signals with (a) no plasma, (b) 10-torr argon discharge, (c) 20-torr argon discharge. Signals are smaller in He plasmas.

The applicable theory is that of Pesme and co-workers [9] for heavily damped ion waves excited in a finite interaction region of length L. The number of e-foldings N above noise is given by

$$N = \frac{\gamma_0^2 L}{c\gamma_i}$$

where γ_0 is the growth rate in an infinite, homogeneous medium, and γ_i is the ion-wave damping rate. This is equivalent to

$$N = 0.1 \frac{n_{16} I_9 L}{T_{ev}} f\left(\frac{T_e}{T_i}\right)$$

where n is the plasma density in units of 10^{16}, I_9 the laser intensity in GW/cm^2, T_{ev} the electron temperature in eV, and $f(T_e/T_i)$ is a function ($\simeq 1$ for $T_e/T_i = 3$) describing ion Landau damping. We estimate $T_e \simeq T_i \simeq 5$-10 eV initially and that T_e is raised to $\simeq 30$ eV by the laser light in the first few nanoseconds. The aforementioned parameters then give $N \simeq 10$, a reasonable value for the observed threshold. This experiment was performed by J.J. Turechek, N. Luhmann, Jr., and F.F. Chen.

ACKNOWLEDGEMENTS

This research was supported by TRW Systems Independent Research and Development funds and at UCLA by the Air Force Office of Scientific Research. The laser work was supported by the USAEC.

REFERENCES

[1] WONG, A.Y., STENZEL, R.L., ARNUSH, D., FRIED, B.D., KENNEL, C.F., REIM, H., Bull. Am. Phys. Soc. 17 (1972) 1017.
[2] STENZEL, R.L., WONG, A.Y., KIM, H.C., Phys. Rev. Lett. 32 (1974) 654.
[3] KIM, H.C., STENZEL, R.L., WONG, A.Y., Phys. Rev. Lett. 33 (1974) 886.
[4] WONG, A.Y., STENZEL, R.L., TRW Systems Research Group Report (Sep. 1974).
[5] OKEZI, H., NISHIKAWA, K., Institute of Plasma Physics, Nagoya University, Research Rep. IPPJ-185 (1974).
[6] MORALES, G., LEE, Y.C., UCLA Plasma Physics Group Rep. 190 (1974).
[7] DRAKE, J.F., KAW, P.K., LEE, Y.C., SCHMIDT, G., LIU, C.S., ROSENBLUTH, M.N., Phys. Fluids 17 (1974) 778.
[8] FORSLUND, D.W., KINDEL, J.M., LINDMAN, E.L., Phys. Rev. Lett. 30 (1973) 739.
[9] PESME, D., LAVAL, G., PELLAT, R., Phys. Rev. Lett. 31 (1973) 203.